Double diaphragm forming simulation for net-shape component using multi-layered biaxial non-crimp fabrics

Fei Yu[1a*], Xiangming Chen[1b*], Shuai Chen[2a*]

[1]Aircraft Strength Research Institute of China, AVIC, Xi'an 710065, China

[2]Composites Research Group, University of Nottingham, Nottingham, UK

[1a*]yuf078@avic.com, [1b*]asrichenxm@avic.com, [2a*]shuai.chen@nottingham.ac.uk

Abstract—Compared to autoclave-cured prepreg, liquid composite moulding (LCM) is a cost-effective alternative to produce advanced composites, thanks to the less-expensive intermediate materials, lower capital investment and shorter cycle time. A separate preforming step is typically required within the process chain to convert 2D fabric blanks into complex 3D geometries before moulding. Numerical models are therefore important to ensure near net-shape preforms during the design phase, in order to minimise the material wastage related to preforming. In this study, a microscale finite element (FE) model was employed to assist in determining the ply shape of multi-ply biaxial non-crimp fabrics (NCF) to achieve net-shape preforms made by double diaphragm forming (DDF) using a spar-like geometry. The forming deformation of the NCF was predicted by simulations considering the in-plane stiffness of the NCF. The location of wrinkles was indicated by the simulation using membrane elements. By continuously removing the redundant fabric material making contact with the machine bed and tool surface, net-shape preforms were achieved for the target geometry using single and multiple NCF plies respectively. Compared with the original ply shape, the number of wrinkles was reduced for the net-shape case due to the reduction in the bridging force induced by the contact pairing between fabric-diaphragm assembly and the machine bed.

1. Introduction

Double Diaphragm Forming (DDF) employs the vacuum forming force to deep-draw the diaphragm-fabric arrangement over a male tool to achieve target geometries, large components can therefore be produced without using oversized hydraulic presses or autoclaves. Both thermoplastic [1] or thermoset prepregs [2] and binder-stabilised dry fabric preforms [3] have been used in DDF to directly manufacture composite components. Two layers of elastomer sheets are typically used during the DDF process to encapsulate the fabric plies with thermoplastic or thermoset binders. The diaphragm-fabric assembly is evaluated of air to provide clamping force on the fabric plies, in order to prevent unwanted ply wrinkling. A rigid frame is typically employed to constrain the diaphragms around their perimeter. The frame is the lowered to drive the fabric-diaphragm arrangement to make contact with the tooling block. A vacuum is subsequently generated between the lower diaphragm and machine bed to create a pressure differential to deep-draw the fabric-diaphragm assembly over the male tool. This vacuum is then maintained to hold the preform, with heating applied to the preform to active the binder. Once the binder has consolidated, the lower vacuum is released for part ejection. The DDF process can be automated to deliver net-shape preforms with repeatable quality, but wrinkling or bridging defects can occur during the process, which limits the practical used of DDF.

Material wastage can be easily minimised by tailoring the initial shape of the fabric prior to forming, as the frictional force at material interfaces is related to the contacting area at fabric-diaphragm interface. It is therefore vital to use simulation tools to determine the perimeter shape of fabrics during the design phase, in order to ensure net-shape preforms. Whilst current studies have focused on the forming behaviour of plies at the same orientation [3], relatively little attention has been paid to determining parameters for net-shape preforming using multi-layered fabric plies at dissimilar orientations.

In this paper, a numerical model for DDF simulation has been developed based on finite element method to model diaphragm forming of biaxial non-crimp fabrics (NCF). A curved spar geometry is used for numerical study and results are presented to demonstrate the strategy for determining the ply shape to enable net-shape preforms produced by DDF using multi-layered biaxial NCFs. The method can be extended to producing component with more complex features.

2. Process simulation

2.1. Material model

Whilst models considering fabric bending stiffness enable explicit prediction for the detailed shape of fabric wrinkling during forming [4], forming simulations using these models typically require impractical runtime due to the large scale of the FE model and a large number of integration points. In comparison, membrane-element-based models are typically computationally inexpensive due to the reduction in the DOFs and integration points in the element formulation. Therefore, the membrane-element-based model developed in [5] was employed in this study to determine the perimeter shape of fabrics to achieve net-shape preforming. A non-orthogonal constitutive model developed in [5, 6] was employed to track the rotation of primary yarns, defining the in-plane shear behaviour of the biaxial NCF, as shown in Fig. 1. In Abaqus/Explicit, the Green-Naghdi (GN) frame is typically established at each integration point to supply the strain increment. In the non-orthogonal framework, the constitutive relation is defined in the yarn parallel system, with the stress contribution of each yarn transformed back to the GN frame at each integration point. Therefore, the fibre re-orientation can be tracked during forming, whilst updating the in-plane shear compliance as the fabric undergoes in-plane shear deformation. The constitutive model was implemented into simulation framework via a Abaqus/Explicit user material subroutine (VUMAT). Since the bending stiffness was overlooked, the shape of forming related wrinkles will be not accurately predicted.

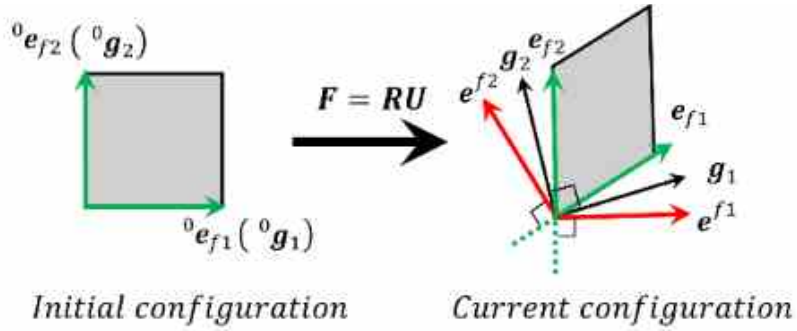

Fig. 1 Schematic of a biaxial fabric unit cell during in-plane shear deformation.

The mechanical properties of the biaxial NCF, characterised in [4, 5], was employed to support the simulation in this study. Two layers of non-crimped fibres in 24K format are stacked at ±45°, with the stiches running along 0° direction to assemble the biaxial arrangement. Hence, the NCF possesses asymmetric in-plane shear resistance for positive (stitches are in tension) and negative (stiches are under compression) shear due to the pillar stitching pattern. The thickness of the NCF ply is 0.4 mm and the

areal mass is 440 gsm. The diaphragm was modelled as a hyperplastic material using the data published in [7].

2.2. Process modelling

A generic tool comprising a segment of curvilinear cross-section was used in this study, as shown in Fig. 2(a). The tool surface includes a curved cross-sectional path with a radius of 150 mm, which could potentially invoke fabric wrinkling and inter-ply movement for forming multi-orientation layup. The Fabric mesh was sandwiched by the two diaphragms, as shown in Fig. 2(b). The diaphragms were constrained in the x-y plane around the perimeter to model constraints from the forming frame. The male tool and the machine bed were modelled as discrete and analytic rigid body respectively. Interactions at all interfaces were modelled using the penalty contact algorithm with Coulomb friction in Abaqus, using the frictional coefficients (CoFs) measured in [8]. The vacuum between the two diaphragms was modelled using two pressures of equal magnitude (1×10^5 Pa) but opposite directions, as shown in Fig. 2(b). This vacuum-clamping force was applied between times A and B in Fig. 2(c). The fabric-diaphragm assembly was draped over the male tool by applying vertical displacement boundary conditions to the rigid frame until the edge of the lower diaphragm contact machine bed. In order to model the evacuation of air between the lower diaphragm and the machine bed, the pressure applied on the lower diaphragm (i.e. denoted by the yellow arrows in Fig. 2(b)) was reduced to zero to generate a pressure gradient (from time B to C in Fig. 2(c)), which draws the diaphragm assembly into contact with the tool surface.

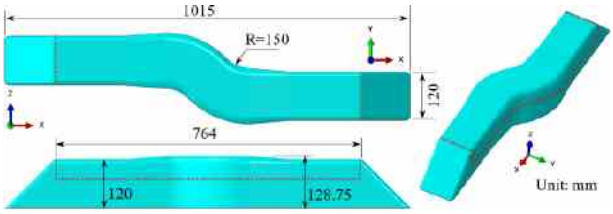

(a)

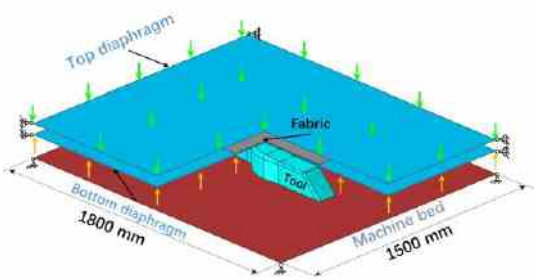

(b)

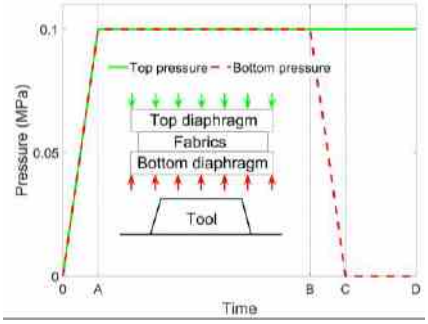

(c)

Fig. 2 (a) Dimensions of the spar-like geometry. The red dotted line denotes the target edge of the perimeter for the final component (b) The configuration of DDF model (c) Diagram illustrating the pressure applied on the diaphragms versus the process time.

3. Net-shape forming

3.1. Methodology

Forming simulations were performed for a single ply (i.e. [-45°/+45°]) and a quad-axial layup (i.e. [-45°/+45°, 90°/0°]) respectively to demonstrate the approach to determining the final shape of the fabric for net-shape forming. The 0° direction is along the length of the spar (X-axis in Fig. 2(a)). The forming simulation was initially performed for a rectangular ply (800 mm × 410 mm, see Fig. 3). Finite elements of the preform located outside the base edge of the tool were removed. Forming simulation was subsequently caried out for the tailored ply shape, with the elements located outside the target trim line (i.e. the red dotted in Fig. 2) of the tool removed to form a new ply shape for next iteration. Multiple

simulations were required to remove the bridging area around the base of the tool to achieve the optimum ply shape. A fixed mass scaling factor was assigned for Abaqus/Explicit solver throughout the forming simulation to reduce run time, with the value of the factor selected to ensure the kinetic energy < 5% of the internal energy throughout the analysis. This ensures the process is simulated as a quasi-static procedure where the inertia effects are negligible compared to the strain energy.

3.2. Results and discussion

Fig. 3 presents the variation of the ply shape during the optimizing process to achieve net-shape preforming for the two cases, where the location of wrinkles correlates with areas of high shear angle. It should be noted that the "wrinkles" predicted by the membrane mesh do not represent the realistic shape of wrinkling defects but may indicate the potential location of these forming related wrinkles.

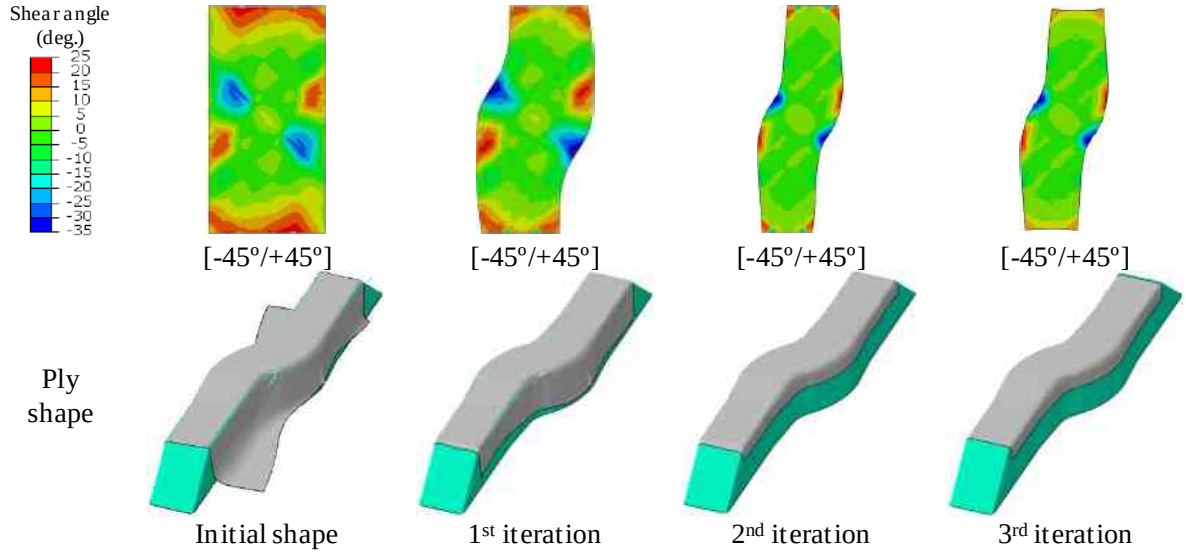

Fig. 3 Simulation results during the iterations for net ply preform (a) A single ±45° NCF ply and (b) A two-ply layup [-45°/+45°, 90°/0°].

For the single-ply case, large bridging defects occur for the initial ply shape (see Fig. 3(a)) due to the large contact area between the fabric/diaphragm assembly and the machine bed. Moreover, wrinkles may occur around the curved areas of the spar. Therefore, the redundant material outside the bridging area has been removed from the fabric, resulting in optimised ply shape. By repeating this procedure, the bridging and wrinkling defects have been eliminated for the final ply shape, indicating the importance of optimising the ply shape in double diaphragm forming. Fig. 4 plots the variation of fibre strains on the undeformed blank during the iteration, where the severity of compressive strain reduces as removing the redundant material. For the initial ply shape and the modified shape after the 1st iteration, wrinkles are found on the convex sides of the tool (see Fig. 3(a)) where the fibres are not under compression, as shown in Fig. 4. This indicates that wrinkles in these areas are more relevant to fabric over-shear (note the high shear regions in Fig. 3(a)). The wrinkles on the concave sides of the tool disappear as modifying the ply shape (see Fig. 3(a)) but high compressive strains remain in these areas (see Fig. 4). This implies that the bridging effects due to the redundant fabric material contribute to the occurrence of these wrinkles.

Similarly, bridging defects are significantly reduced for the quad-axial layup (i.e. [-45º/+45º, 90º/0º]) as the net ply shape changes, but additional wrinkling defects may occur near the doubly-curved features (see Fig. 3(b)) due to the interaction between the two plies of dissimilar shear deformation. The severity of these wrinkles reduces as removing the redundant material due to the reduction in the contact area between the two plies and the bridging force. Fig. 5 presents the distributions of fibre strains overlaid onto the undeformed blank for the quad-axial layup during the iteration. Overall, the areas of fabric with high compressive strain reduce as the removal of redundant fabric materials, which correlates with the reduction in the severity wrinkling defects (see Fig. 3(b)). For all iterations, high tensile strains are seen in the 90º/0º ply due to the bridging of 0º fibres over the concave area of the tool, corresponding to the wrinkles on the concave sides of the tool. Large areas of fibre compression are found in each ply of the preform, indicating that plies at different orientations may compete against each other during forming due to the dissimilar shear deformation of adjacent plies. Whilst the two plies undergo dissimilar shear deformation with respect to the tool, the final shapes required for net-shape preforming for the two plies are almost identical in this case, as show in Fig. 3(b).

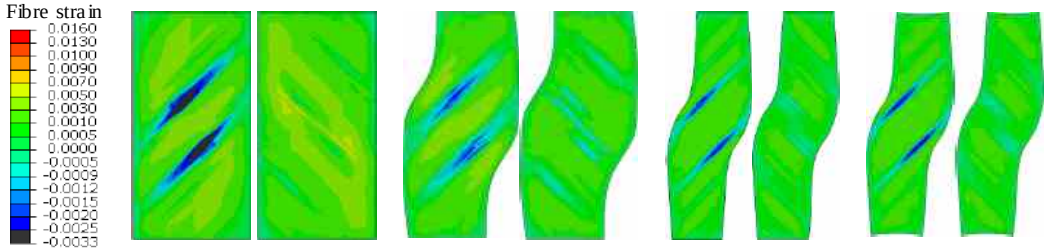

Fig. 4 Variation of fibre strains for the single-ply case (i.e. [-45º/+45º]) during the iteration.

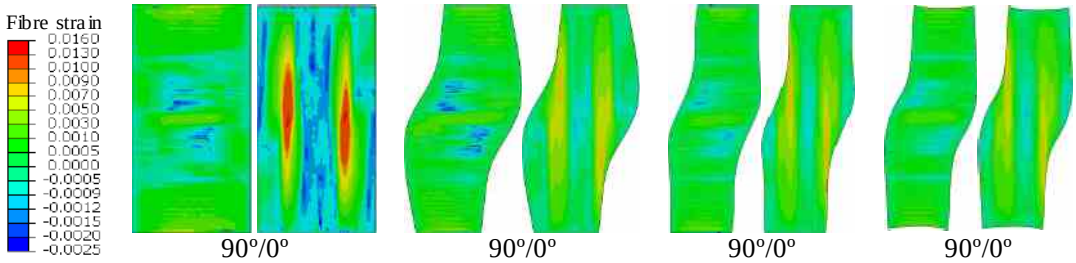

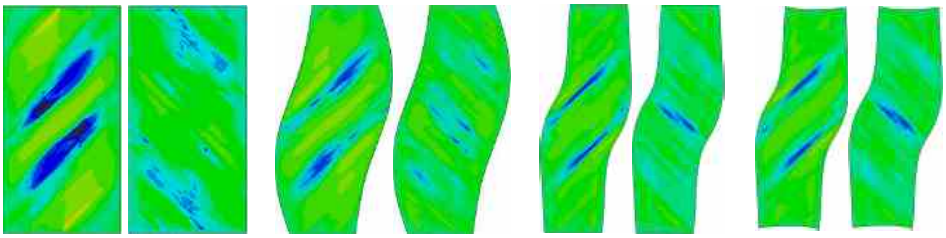

Fig. 5 Variation of fibre strains for the two-ply layup (i.e. [-45°/+45°, 90°/0°]) during the iteration.

4. Conclusion

Based on the results and discussions presented above, the conclusions are obtained as below:

(1) Out-of-plane wrinkling and bridging are the dominant defect for diaphragm forming, as the forming pressures are relatively low (up to 1 bar) compared to matched tool forming.

(2) Redundant fabric material outside the tool provides additional bridging force during diaphragm force, leading to diaphragm pitching and hence fabric wrinkling. The shape of fabric therefore needs to be designed to prevent excessive bridging area around the tooling block to achieve net-shape preform and to reduce defects.

(3) Layups containing multiple ply orientations are more prone to wrinkling defects due to the dissimilar in-plane shear deformation between adjacent plies.

(4) The method described in this paper can successfully identify fabric bridging and determine the fabric shape for net-shape preform, whilst achieving desirable surface conformity.

The future work will be focusing on employing simulation tools considering fabric bending stiffness to provide more confidence on wrinkle prediction, with the aim to explore feasible solutions for defect mitigation.

References

[1] Bersee, H.E.N. and A. Beukers, (2002) Diaphragm forming of continuous fibre reinforced thermoplastics: influence of temperature, pressure and forming velocity on the forming of Upilex-R® diaphragms. Composites Part A: Applied Science and Manufacturing. 33(7): p. 949-958.

[2] Bian, X.X., et al., (2013) Effects of Processing Parameters on the Forming Quality of C-Shaped Thermosetting Composite Laminates in Hot Diaphragm Forming Process. Applied Composite Materials. 20(5): p. 927-945.

[3] Chen, S., et al., (2017) Double diaphragm forming simulation for complex composite structures. Composites Part A: Applied Science and Manufacturing. 95: p. 346-358.

[4] Yu, F., et al., (2020) A macroscale finite element approach for simulating the bending behaviour of biaxial fabrics. Composites Science and Technology. 191.

[5] Chen, S., et al., (2016) Defect formation during preforming of a bi-axial non-crimp fabric with a pillar stitch pattern. Composites Part A: Applied Science and Manufacturing. 91: p. 156-167.

[6] Yu, F., et al., (2021) Simulating the effect of fabric bending stiffness on the wrinkling behaviour of biaxial fabrics during preforming. Composites Part A: Applied Science and Manufacturing: p. 106308.

[7] Yu, F., et al., (2021) Double diaphragm forming simulation using a global-to-local modelling strategy for detailed defect detection in large structures. Composites Part A: Applied Science and Manufacturing. 147: p. 106457.

[8] Yu, F., et al., (2021) Investigation into the effects of inter-ply sliding during double diaphragm forming for multi-layered biaxial non-crimp fabrics. Composites Part A: Applied Science and Manufacturing. 150: p. 106611.